

Statistical Investigations of 1315 Radio Pulsars

O. H. Guseinov^{1,2} *, E. Yazgan² †, S. Özkan¹ ‡, A. Sezer¹ §, and S. Tagieva³ ¶

¹Department of Physics, Akdeniz University,
Antalya, Turkey

²Department of Physics, Middle East Technical University,
Ankara, Turkey

³Academy of Science, Physics Institute Baku 370143,
Azerbaijan Republic

Abstract

In this paper we have used the data of 1315 pulsars (Guseinov et al. 2002) for statistical analysis and showed the changes in pulsar parameters since the appearance of Taylor et al. (1996) catalog. Here we present the space distribution of pulsars, dispersion measures, distances from the galactic plane and from the Sun, electron density, luminosity distributions at 400 and 1400 MHz, the relations between luminosities of pulsars at 400 and 1400 MHz and the dependence of luminosity on age and on magnetic field. We also present the updated P- \dot{P} diagram.

KEY WORDS Pulsars, Compact Stars, Neutron Stars

1 INTRODUCTION

Observational and derived data of radio pulsars (PSRs) were last compiled in 1996 (Taylor et al. Catalog of 706 PSRs, unpublished work). This catalog

*e-mail:huseyin@pascal.sci.akdeniz.edu.tr

†e-mail:yazgan@astroa.physics.metu.edu.tr

‡e-mail:sozkan@pascal.sci.akdeniz.edu.tr

§e-mail:sezer@sci.akdeniz.edu.tr

¶e-mail:SO_Tagieva@mail.ru

has tremendous contributions in the development of PSR astronomy. The first full catalog (Manchester & Taylor 1981) includes 333 PSRs which were discovered before 1981. Many PSRs were discovered after 1981 (Dewey et al. 1985; Stokes et al. 1985, 1986; Clifton et al. 1992; Johnston et al. 1992a,b) and these PSRs were included in the Taylor et al. (1996) catalog.

After the publication of the Taylor et al. (1996) catalog, there have been a number of pulsar surveys (Johnston et al. 1995; Lyne et al. 2000; D’Amico et al. 2001; Edwards & Bailes 2001; Camilo et al. 2000; Manchester et al. 1996; Lyne et al. 1998, Sandhu et al., 1997). Furthermore, the inner parts of SNRs were scanned (completely or partially) to detect PSRs genetically connected with SNRs (Gorham et al. 1996; Kaspi et al. 1996; Lorimer et al. 1998). After 1996, it became more or less certain that the PSR-SNR pairs J2229+6114 – G106.6+2.9 (Halpern et al. 2001), J0205+64 – G130.7+3.1 (Murray et al. 2002), J1846-0258 – G29.7-0.3 (Gotthelf et al. 2000), J1124-5916 – G292.0+1.8 (Camilo et al. 2002), J1119-6127 – G292.2-0.5 (Crawford et al. 2001; Pivovarov 2001), J1803-2137 – G8.7-0.1 (Kassim & Weiler 1990, Finley & Oegelman 1994) and J1952+3525 – G69.0+2.7 (Strom 1987, Shull et al. 1989) possibly have genetic connections (Allakhverdiev et al. 1997, Kaspi & Helfand 2002). Also, there have been searches for PSRs in Globular Clusters (GC) (Camilo et al. 2000; D’Amico et al. 2001; Lyne 1995; Kulkarni & Anderson 1996; Biggs and Lyne 1996). Before 1996, 10 PSRs were detected in GC NGC104 (47 Tuc) and after 1996, 10 new pulsars have been detected in this GC (Camilo et al. 2000). No new PSRs have been found from other GCs which have PSRs detected before 1996. After 1996, one PSR for each of the following GCs were detected; NGC 6266, NGC 6342, NGC 6397, NGC 6544 and NGC 6752. However, the available catalog (Taylor et al. 1996) has not been updated since then.

Earlier, most of the PSRs were discovered at 400 MHz and frequencies close to 400 MHz. Since the dispersion measure (DM) of distant PSRs are larger, new PSR surveys and searches in SNRs and GCs have been conducted at 1400 MHz to obtain narrow pulses. Observations at 1400 MHz are also necessary for the study of other parameters of PSRs such as the spectral index. As expected, most of the new detections of PSRs were in the Galactic center direction. After 1996 no PSRs have been detected in the Magellanic Clouds (MC), except one PSR which has a period of 16 ms (PSR J0537-6910) detected in SNR N157B in the Large Magellanic Cloud (LMC), in the X-ray band (Marshall, Gotthelf, Zhang et al. 1998; Mignani, Pulone, Marconi et al. 2000). The reason for this PSR not to be seen in the radio band might be that it might have a medium radio luminosity.

The number of PSRs detected in GCs increased by a factor of 1.5. The number of millisecond PSRs ($P < 0.1$ sec and $\dot{P} < 10^{-16}$ s/s) whose period and period derivative values are known, increased more than 1.5 times. The number of PSRs with low flux have considerably increased as a result of more (spatially) precise scans with high sensitivity. In the Arecibo window ($40^\circ < l < 65^\circ$; $|b| < 2.5^\circ$) (Hulse & Taylor 1974, 1975), 12 new PSRs are discovered.

Guseinov et al. (2002) compiled observational and derived data for 1315 PSRs. The purpose of this work is to perform statistical analysis using these data. Statistical investigations of PSRs have an important role in understanding their physical properties and origin. But today radio pulsars are not the unique phenomenon for neutron stars. Unexpected but very important discovery of the soft gamma repeaters and the related objects, anomalous X-ray pulsars, showed us that we have problems in understanding neutron stars as a whole class. The different NS types might be due to the differences of their progenitor stars which we do not know very clearly. Statistical investigations of PSRs will help to understand the whole family of neutron stars.

2 SPACE DISTRIBUTION OF PULSARS

The distribution of 1315 PSRs in the Galaxy with respect to Galactic longitude (l) and latitude (b) is displayed in Figure 1a. Comparing the new distribution with the space distribution of PSRs known before 1996 (Gök et al. 1996) we see that at high latitude ($|b| > 10^\circ$) many new PSRs have been detected both in the Northern and Southern sky. Naturally, many new PSRs are detected in the spiral arms and galactic center directions. If we compare the l - b distribution of 862 galactic PSRs in Figure 1b which have flux values measured at 1400 MHz, with the l - b distribution for PSRs with known flux at 400 MHz (Gök et al. 1996) then we see that for many PSRs with high galactic latitude, 1400 MHz flux values have been measured after 1996. But comparison of Figure 1a and 1b shows that still for many PSRs (453 of them) especially at high latitudes, the 1400 MHz flux are not known yet. From these two figures, it is also seen that 1400 MHz flux values for some of the PSRs on the Galactic Plane are not known. The PSRs without 1400 MHz flux are the ones whose 400 MHz flux are lower. In Figure 1b PSR J1239+2453 ($l=252.4^\circ, b=86.5^\circ$) has the highest galactic latitude b and PSR J0134-2937 ($l=230.2, b=-80.2$) has the lowest value of b . These PSRs

respectively have distances of 0.56 kpc and 1.5 kpc and luminosities of 34.5 mJy kpc² and 20.2 mJy kpc² at 400 MHz, 3.13 mJy kpc² and 5.39 mJy kpc² at 1400 MHz (Guseinov et al. 2002).

Figure 1c displays the l-b distribution of 420 PSRs discovered after 1996 with known 1400 MHz flux. As seen from the figure, after 1996, in the southern hemisphere of the Galaxy more PSRs have been discovered. Moreover, it is seen that, survey of the arms of the Galaxy in the galactic center direction has been more precise. In this figure J1313+0931 (l=320.4°, b=71.7°) has the highest galactic latitude and J2346-0610 (l=83.9°, b=-64.8°) has the lowest latitude. The distances of these PSRs are respectively 0.6 and 1.9 kpc, the luminosities at 400 MHz are 1.26 and 39.72 mJy kpc² and at 1400 MHz are respectively 0.057 and 7.23 mJy kpc².

Before, the most precisely scanned region of the Galaxy was the Arecibo window (Hulse & Taylor 1974, 1975). Up to 1996, in this region, 48 PSRs had been discovered. Now the number of PSRs in this region is 60. For these recently discovered 12 PSRs, the flux values at 1400 MHz are less than or equal to 0.5 mJy. One of these PSRs, namely PSR J 1907+0918 (l=43.02°, b=0.73°) has a highly flat spectrum (F₄₀₀=0.4 mJy, F₁₄₀₀=0.3 mJy). This PSR is located at a distance of 7.67 kpc and have luminosities of L₄₀₀=23.5 mJy kpc² and L₁₄₀₀=17.7 mJy kpc². For the other 11 PSRs flux values at 400 MHz do not exist in Guseinov et al. (2002). For the 48 PSRs discovered before, only 4 of them have flux values at 400 MHz lower than 1 mJy. These data show that, even though the survey is thorough, precise and scanning is conducted at a higher frequency, it is hard to detect new PSRs in this region.

The whole Arecibo window had not been scanned with the same quality before. The best scanned region was 43° <l<55° (Hulse & Taylor 1974, 1975). Now the longitudes are scanned more precisely. Therefore it is natural that most of the recently discovered PSRs have galactic longitude values between 40° and 46° and most of them lie near to 40°.

Figure 2a displays the DM values of 1312 PSRs in the Galaxy with respect to galactic longitude. None of the DM values of PSRs discovered up to 1996 (except PSR J 1801-2306 (l=6.8°, b=-0.8°) which has DM=1074 cm⁻³ pc) do not exceed 800 cm⁻³ pc. Only 7 PSRs have DM>600 cm⁻³ pc in Taylor et al. (1996) catalog. But now, as seen from Figure 2a, 83 PSRs have DM>600 cm⁻³ pc and 31 PSRs have DM>800 cm⁻³ pc. These, naturally, are located at the arms close to the Galactic center. Four PSRs have DM>1100 and are located in 330° <l<337°. Among these four PSRs, the one with the highest DM value (DM=1209 cm⁻³ pc) is PSR J 1628-4848 (l=335.5°, b=0.2°). The

PSRs named in Figure 1: PSR J1801-2306 ($l=6.8^\circ, b=-0.8^\circ$), PSR J2044+46 ($l=85.4^\circ, b=2.1^\circ$), PSR J0631+1036 ($l=201.2^\circ, b=0.5^\circ$), PSR J0855-4658 ($l=267.3^\circ, b=-1^\circ$) and PSR J1019-5749 ($l=283.8^\circ, b=-0.7^\circ$) have the largest DM values in their own directions.

Figure 2b displays the distance from the galactic plane (Z) versus DM for 1273 PSRs with $|Z| < 2$ kpc. The 83 PSRs having DM greater than 600 are all in Figure 2b. The distances of these PSRs from the Galactic plane, do not exceed 320 pc (Compare Figures 2a and 2b). The reason that the PSRs with high DM value have such low $|Z|$ values is that the new surveys are focused on low galactic latitudes. However, even if high Galactic latitudes were scanned, we would not expect to find the ratio of PSRs with DM values greater than $600 \text{ cm}^{-3} \text{ pc}$ to all PSRs to change considerably. Because, as we move away from the galactic plane, electron density decreases abruptly. The PSRs, which are the members of the Galaxy but far away from the galactic plane, are located in GCs. Among these, the highest one from the galactic plane is PSR J1312+1810 ($l=332.9, b=79.8$) and have $Z=18.6$ kpc.

Figure 3a represents the distances of 1307 PSRs which belong to our Galaxy versus galactic longitude (l). The farthest PSR from the Solar system is PSR J1312+1810. This PSR is a member of the globular cluster M53 which have a very small value of $DM=24 \text{ cm}^{-3} \text{ pc}$. The name of the most distant PSRs for several different longitude intervals are indicated in Figure 3a. These galaxy field PSRs (which do not belong to GCs) with distances $d > 10$ kpc are all located close to the galactic plane (compare Figures 3a and 2b). The PSRs with largest values of DM (Figure 2a) added here are mentioned before as the PSR in M53 and PSR J1305-6256 ($l=304.5^\circ, b=-0.1^\circ$).

Figure 3b represents the projection of the location of PSRs on the plane of the Galaxy. In this figure, the distance between consecutive rings is 2 kpc. From the figure it is seen that behind the Galactic center ($l \approx \pm 10^\circ, d > 8.5$ kpc) there are not many PSRs with large distances similar to the PSRs, for example, in the direction $l=300^\circ-310^\circ$. The most important reason is that near the Galactic center the background radiation is strong. Moreover as the distance of the PSR increases, DM increases, flux decreases and the *observed* pulse width increases. Therefore it is hard to find such PSRs beyond the Galactic center. For the distant PSRs in this direction, the DM values are not as high as the ones at $l=340^\circ$ (see Figure 2a) since background radiation do not let us see such distant PSRs even though their luminosity are large enough to be seen if they were not located near the center direction.

Only old population stars (stars with ages about 10^{10} years) can come

to dynamical stability. But old and young populations are not in dynamical equilibrium with each other, because the scale height and density distributions of the two populations are different. The total mass of gas and young stars located in the Galactic arms is only about 1% of the mass of the whole Galaxy and the parameters of these arms change with time. SFRs are yet more unstable having ages about an order of magnitude less than the characteristic ages of the arms of the Galaxy. Here, the arms are neither in dynamical equilibrium with the Galaxy, nor with the SFRs. Therefore not in all regions on the geometrical plane, arms must be coincident with the geometrical plane of the Galaxy. For some regions SFRs may be higher or lower from the plane of the the Galaxy. From optical observations of cepheids with high luminosities (with long pulsation periods) and red supergiants, which are located at distances about 5-10 kpc from the Sun, it is found that, in the direction $l=220^{\circ}$ - 330° , SFRs lie about 300 pc below the galactic plane. In the same distance, in the direction $l=70^{\circ}$ - 100° it is found that SFRs lie about 400 pc above the galactic plane, and the young objects closer than 3-5 kpc in the direction $l=270^{\circ}$ - 320° are located about 150 pc down the geometrical plane of the Galaxy (Berdnikov 1987).

Figure 4a displays the distribution of the distance of 1307 galactic PSRs from the plane of the Galaxy as a function of galactic longitude. Due to the fact that the PSRs in GC M5 ($l=3.9^{\circ}$, $b=46.8^{\circ}$, $d=9$ kpc), M13 ($l=59.8^{\circ}$, $b=40.9^{\circ}$, $d=7.7$ kpc), M53 ($l=332.9^{\circ}$, $b=79.8^{\circ}$, $d=18.9$ kpc), M15 ($l=65.1^{\circ}$, $b=-27.3^{\circ}$, $d=10$ kpc) and 47 Tuc ($l=305.9^{\circ}$, $b=-44.9^{\circ}$, $d=4.5$ kpc) have $|Z| > 3$ kpc, they are plotted at closer distances than their real distance values. (There is one PSR known in M53, 2 in M5, 2 in M13, 8 in M15 and 20 in 47 Tuc). In Figure 4a, the values of distances of these PSRs from the plane of the Galaxy are shown. Naturally, the PSRs with low flux are not scanned thoroughly with the same precision on all of the sky. This and the deviation of the SFRs from the galactic plane affect mostly the distant PSRs which are located in the peripheric parts of the Galaxy, so we have plotted the Z-l distribution of 551 PSRs with $d > 5$ kpc in Figure 4b. As it is seen from the figure, expectedly, the PSRs in the direction $l=70^{\circ}$ - 100° are generally located above the galactic plane and the PSRs in the direction $l=200^{\circ}$ - 300° are located below the Galactic plane. Among these PSRs J1721-1936 ($l=4.9^{\circ}$, $b=9.7^{\circ}$), J0952-3839 ($l=268.7^{\circ}$, $b=12.3^{\circ}$) and J0745-5351 ($l=266.6^{\circ}$, $b=-14.3^{\circ}$) have the largest deviations from the plane of the Galaxy and they have distances of 9, 7.2 and 6.2 kpc, respectively.

Figure 5 represents the average value of electron density, n_e , along the line of sight as a function of galactic longitude (1312 PSRs; 5 PSRs in MCs

are included). PSR J1818-1519 ($l=15.6^\circ$, $b=0.1^\circ$, $n_e=0.085 \text{ cm}^{-3}$) has a distance of 8.2 kpc, J0826+2637 ($l=196.9^\circ$, $b=31.7^\circ$, $n_e=0.049 \text{ cm}^{-3}$) has $d=0.4$ kpc, PSR J0828-3417 ($l=253.9^\circ$, $b=2.6^\circ$, $n_e=0.039 \text{ cm}^{-3}$) has $d=1.2$ kpc, PSR J1119-6127 ($l=292.2^\circ$, $b=-0.54^\circ$, $n_e=0.094 \text{ cm}^{-3}$) has $d=7.5$ kpc, PSR J1302-6350 ($l=304.2^\circ$, $b=-0.9^\circ$, $n_e=0.113 \text{ cm}^{-3}$) has $d=1.3$ kpc, PSR J1644-4559 ($l=339.2^\circ$, $b=-0.2^\circ$, $n_e=0.107 \text{ cm}^{-3}$) has $d=4.5$ kpc. PSR J0835-4510 ($l=263.6^\circ$, $b=-2.8^\circ$) in Vela SNR has the highest value of $n_e=0.15 \text{ cm}^{-3}$. This value is found by assuming the distance to the PSR to be $d=0.45$ kpc. In the following paragraph we explain our reasons to take the distance to Vela to be 0.45 kpc.

The distance to the Vela remnant is given as $d=250$ pc (Ögelman et al. 1989), $d=250\pm 30$ pc (Cha et al. 1999; Danks 2000), $d\approx 280$ pc (Bocchino et al. 1999). But we have to take into account the fact that Vela SNR is expanding in a dense medium. The magnetic field is given as 6×10^{-5} Gauss (de Jager et al. 1996) and as $(5-8.5)\times 10^{-5}$ Gauss (Bocchino et al. 2000) and explosion energy is $(1-2)\times 10^{51}$ ergs (Danks 2000). These values are more than the average. Naturally, the errors are high for these quantities. However, if we assume that these data are correct and the distance to the Vela remnant is 250 pc, then in Σ -D diagram Vela and the SNR G 327.6+14.6 are located at the same position. However, this is not convincing, since Vela and SNR G 327.6+14.6 are formed from different type of SN explosions, i.e. SNR G 327.6+14.6 was formed from a type Ia explosion (Hamilton et al. 1997). This SNR has a distance of 500 pc from the galactic plane, and consequently it lies in a much less dense medium than the medium of Vela remnant. And in the Σ -D diagram it is hard to understand the deviation of the Vela remnant from the Σ -D relation. On the other hand, the deviation of SNR G 327.6+14.6 is readily understandable, because this SNR is formed from a type Ia explosion, but the Σ -D relation is for S and C-type SNRs. The distance of OB associations including the young open clusters (OC) in the direction of Vela remnant are not closer than 0.25 kpc. One of these OCs which lie in the OB association (OB2) closer to the Sun, in the direction of Vela, is Pismis 4 ($l=262.7^\circ$, $b=-2.4^\circ$). Pismis 4 has a well known distance of 0.6 kpc. (Ahumada & Lapasset 1995; Aydın et al. 1997). Since the progenitors of SNRs (or pulsars) are massive stars, the probability that Vela is not at 0.25 kpc but closer to the SFR is high. As seen from Figure 5, PSR J1302-6350 has the second highest n_e (after Vela) which is 0.113 cm^{-3} is PSR J1302-6350 ($l=304.2^\circ$, $b=-0.9^\circ$) which has a Be star companion (having a variable wind) and which is at a distance of 1.3 kpc (Johnston et al. 1994). So, it is normal for this PSR to have such a

high n_e . The third highest n_e is 0.107 cm^{-3} which is calculated for PSR J 1644-4559 ($l=339.2^\circ, b=-0.2^\circ$). Since the luminosity at 1400 MHz for this last PSR is higher than all other PSRs with known flux ($L_{1400}=6.3 \times 10^3$, $L_{400}=7.9 \times 10^3$, see Figure 6b), it would not be true to accept its distance to be more than 4.5 kpc. PSR J1341-6220 ($l=308.7^\circ, b=-0.4^\circ$) has $n_e=0.091$ (which is the fourth highest n_e) at $d=8$ kpc. For SNR G308.8-0.1 which is thought to be genetically connected with this PSR, the angular size and flux value are not precisely known. But we cannot accept that this SNR is located farther. Due to these reasons the distance to the PSR-SNR pair must be about 8 kpc (Using the Σ -D diagram of Guseinov et al., in preparation). In the direction and distance of this PSR, SFR lies below the galactic plane. Consequently, n_e shows asymmetric distribution about the plane, and the value of n_e below is higher than the corresponding n_e at the same longitude with same b value but above the plane. For all of the PSR sample, average value of n_e is around 0.04 cm^{-2} . Using 250 pc for the distance of Vela leads to an electron density two times higher than the electron density calculated assuming the distance to be about 400 pc. However, even when the distance is assumed to be 400 pc, n_e is readily the highest of all. So distance to Vela is at least 0.4 kpc and the most recent SNR catalog (Green, 2001) gives the distance to Vela as ~ 0.5 kpc.

The value of the electron density along the line of sight is high for the Vela PSR because it lies in an SNR in the nearest OB association. There are about 15 PSRs genetically connected to SNRs in our Galaxy (Kaspi & Helfand 2002). Some of these SNRs with high probability lie in OB associations. However, since these associations are distant sources (so column depth is high), value of n_e along the line of sight is less.

Figure 6a displays the luminosity at 400 MHz ($L_{400}=F_{400}d^2 \text{ mJy kpc}^2$) with respect to longitude for 685 PSRs. For 12 PSRs $\text{Log } L_{400} < 0$ and 10 of these PSRs lie in $0^\circ < l < 150^\circ$. This is because the Arecibo survey scanned the northern sky more thoroughly with very high sensitivity. The PSRs with least L_{400} are J0108-1431 ($l=140.9, b=-76.8$) and J0006+1834 ($l=108.2, b=-42.9$). They respectively have distances of 0.08 kpc and 0.7 kpc and luminosity values of 0.058 mJy kpc^2 and 0.098 mJy kpc^2 . The strongest PSRs at 400 MHz are respectively J0529-6656 ($l=272.2, b=-32.8$) belonging to the LMC, J0738-4042 ($l=254.2, b=-9.2$) and J1901+0331 ($l=37.2, b=-0.6$). These have distances of 50, 8 and 8.03 kpc respectively. Luminosity values of these PSRs at 400 MHz are $1.37 \times 10^4 \text{ mJy kpc}^2$, $1.28 \times 10^4 \text{ mJy kpc}^2$ and $1.06 \times 10^4 \text{ mJy kpc}^2$, respectively.

In Figure 6b the luminosity at 1400 MHz versus longitude for 862 galactic

PSRs are displayed. At these frequencies, the galactic plane is scanned with high sensitivity, and also the flux of closer PSRs which have known values at 400 MHz are measured. From the fact that on the average the flux of PSRs at 400 MHz is about 6-7 times more than the flux at 1400 MHz, it could be inferred that the PSRs with $\text{Log } L_{400} < 1$ will have values of $\text{Log } L_{1400} < 0$. For some of these PSRs (with $\text{Log } L_{400} < 1$) values of F_{1400} are unknown. The number of PSRs with $\text{Log } L_{1400} < 0$ is 42 and naturally most of them have high galactic latitudes since background radiation is low at high galactic latitudes (for approximately 30 of them, $|b| > 5^\circ$). PSRs J0030+0451 ($l=113.1^\circ$, $b=-57.6^\circ$) and J2144-3939 ($l=2.7^\circ$, $b=-49.5^\circ$) have the lowest values of luminosity at 1400 MHz. They respectively are located at distances of 0.235 and 0.2 kpc and have $L_{1400}=0.033$ and 0.032 mJy kpc². The strongest PSRs at 1400 MHz are J1644-4559 ($l=339.2^\circ$, $b=-0.2^\circ$), J0738-4042 ($l=254.19^\circ$, $b=-9.19^\circ$), J1935+1616 ($l=52.4^\circ$, $b=-2.9^\circ$) and J1243-6423 ($l=302.5^\circ$, $b=-1.5^\circ$) PSR J0738-4042 has a large luminosity also at 400 MHz. But these PSRs are not related to the PSRs which we have mentioned as the farthest PSRs in Figure 3a, i.e. the farthest PSRs do not necessarily have the highest luminosities; we can observe the farthest ones because they have high galactic latitudes, and the OCs are scanned thoroughly. These PSRs respectively have distances of 4.5, 6.2, 8.3 and 9 kpc and luminosities at 1400 MHz 6.29×10^3 , 5.5×10^3 , 1.61×10^3 and 1.63×10^3 mJy kpc².

3 Luminosities of PSRs at 400 and 1400 MHz

Figure 6c displays $\text{Log } L_{1400}$ versus $\text{Log } L_{400}$ values. The number of PSRs with known values of flux both at 400 and 1400 MHz simultaneously is 449. The relation between L_{1400} and L_{400} we infer from these PSRs in Figure 6c is

$$L_{1400} = 0.1L_{400}^{1.0 \pm 0.1} \quad (1)$$

PSRs have radio spectral index values, on the average, that the flux at 1400 MHz is about 6.3 times less than the flux at 400 MHz. As seen from Figure 6c, some PSRs deviate strongly from the relation in Equation 1. For example, J1302-6350 ($l=304.2$, $b=-0.9$) which has a Be star companion has $L_{1400}/L_{400}=1.35$. For PSR J1114-6100 ($l=291.4^\circ$, $b=-0.3^\circ$) value of $L_{1400}/L_{400}=1.16$, for PSR J1633-4805 ($l=336.3^\circ$, $b=-0.11^\circ$) value of $L_{1400}/L_{400}=0.005$. For the PSR J1644-4559 ($l=339.2^\circ$, $b=-0.2^\circ$) which has the highest luminosity among all PSRs at 1400 MHz, value of $L_{1400}/L_{400}=0.83$.

Characteristic ages of these PSRs are respectively equal to 3.3×10^5 yr, 2.9×10^7 yr, 3×10^5 yr, 1.4×10^5 , and 3.5×10^5 yr.

In Figure 7a luminosity values of PSRs at 1400 MHz versus their characteristic ages (Log L_{1400} -Log τ diagram) for 853 PSRs (5 PSRs in MC are included) is displayed. From the figure it is seen that for PSRs whose Log $\tau > 6.5$, luminosity decreases as τ increases. Here, the effect of millisecond PSRs is strong. The luminosity of young PSRs, practically, do not depend on τ .

In Figure 7b, luminosity at 1400 MHz versus magnetic field (Log L_{1400} -Log B diagram) for the same 853 PSRs is given. Magnetic field is calculated from the well-known relation $B = 3.3 \times 10^{19} (P\dot{P})^{1/2}$. As seen from the figure the luminosity of PSRs, including millisecond PSRs with magnetic fields less than 3×10^{10} Gauss have considerably low luminosity values, on the average, than luminosities of young PSRs (i.e. $B > 3 \times 10^{11}$ G). As seen from the figure the PSRs with magnetic fields about 10^{12} Gauss can have luminosity values in a 5 order interval. Such PSRs with high magnetic fields can also have low luminosities like millisecond PSRs have. As inferred from Figure 7a and b the huge difference in the luminosities of PSRs are innate. Most of the PSRs are born single. In Figure 8a Log L_{1400} -Log L_{400} diagram for single PSRs with $\tau < 10^7$ years is represented. For the 273 PSRs in this figure, the relation between L_{1400} and L_{400} is found as

$$L_{1400} = 0.17 L_{400}^{0.99 \pm 0.1} \quad (2)$$

From figures 6c and 8a we see that spread in the luminosities of young PSRs may be large (see the errors in slopes of expressions (1) and (2)). From Figures 6c and 8a we also see that PSRs with luminosities $L_{400} < 30$ mJy kpc² are in average considerably softer (L_{1400}/L_{400} is small) than PSRs with higher luminosity values. Since PSRs are non-stationary objects, their flux and spectral index can change in time. To have confidence, we have plotted Log L_{1400} -Log L_{400} diagram for PSRs with $\tau < 10^6$ years (Figure 8b). The degree of dependence inferred from this figure:

$$L_{1400} = 1.15 L_{400}^{0.72 \pm 0.05} \quad (3)$$

for PSRs with $\tau < 10^6$ years is considerably less.

Radio luminosity and spectral properties of neutron stars are very important also for investigation of AXPs, SGRs and DRQNSs. So we have also investigated L_{1400} - L_{400} dependence on magnetic field strength. However, we found that the slope of L_{1400} - L_{400} do not depend on magnetic field strength.

Evidently, there can be huge uncertainties in the flux measurements (especially when the flux is low). Because of these reasons, even though we do not consider the distance errors, the location of several PSRs can change in Figures 6c, 8a and 8b. However, we do not expect the Equations 1, 2 and 3 to change, since the number of data is high enough.

The P- \dot{P} diagram is displayed in Figure 9. In this figure constant characteristic age line, constant magnetic dipole field lines and the constant rate of rotational energy loss lines are also plotted. The rate of rotational energy loss \dot{E} is calculated from the formula $\dot{E}=3.94 \cdot 10^{46} \dot{P}/P^3$. As expected, the form of the diagram changed as the number of data increased.

4 Discussion and Conclusions

As the number of PSRs increases, we understand the physical properties of neutron stars more clearly, parameters of PSRs are better determined and the distances become more reliable. Therefore, our knowledge about PSRs considerably increased from their space-kinematic characteristics to their physical properties. It is especially necessary to note that the increase of our knowledge is due to the precise observations at 1400 MHz.

Acknowledgements. We thank TÜBİTAK, the Scientific and Technical Research Council of Turkey, for support through TBAG-ÇG4.

References

- Ahumada, J., Lapasset, E., 1995, *A&AS*, 109, 375
- Allakhverdiev et al. 1997, *Turkish Journal of Physics*, 21, 688
- Aydın, C., Albayrak, B., Gözel, I., Guseinov, O.H., 1997, *Turkish Journal of Physics*, 21, 875
- Berdnikov, L.N., 1987, *Soviet Astronomy Letters*, 13, 45
- Biggs, J.D., & Lyne, A.G., 1996, *MNRAS*, 282, 691
- Bocchino, F., Maggio, A., Sciortino, S., 1999, *A&A*, 342, 839
- Bocchino, F., Maggio, A., Sciortino, S., and Raymond, J., 2000, *A&A*, 359, 316
- Camilo, F., Lorimer, D.R., Freire, et al. 2000, *ApJ*, 535, 975
- Camilo, F., Manchester, R.N., Gaensler, B.M., et al. 2002, *ApJ*, 567, L71
- Cha, A.N., Sembach, K.R., Danks, A.C., 1999, *ApJ*, 515, L25
- Clifton, T.R., Lyne, A.G., Jones, A.W., et al. 1992, *MNRAS*, 254, 177
- Crawford, F., Gaensler, B.M., Kaspi, V.M., et al. 2001, *ApJ*, 554, 152
- D'Amico, N., Lyne, A.G., Manchester, R.N., et al. 2001, *ApJ*, 548, L171
- Danks, A.C., 2000, *Ap&SS*, 272, 127
- De Jager, O.C., Harding, A.K., Strickman, M.S., 1996, *ApJ*, 460, 729
- Dewey, R.J., Taylor, J.H., Weisberg, J.M., Stokes, G.H., 1985, *ApJ*, 294, L25
- Edwards, R.T., Bailes, M., 2001, *ApJ*, 553, 801
- Finley, J.P., & Oegelman, H., 1994, *APJ*, 434, 125
- Gök, F., Alpar, M.A., Guseinov, O.H., Yusifov, I.M., 1996, *Turkish J. Phys.*, 20, 275
- Gorham, P.W., Ray, P.S., Anderson, S.B., et al. 1996, *APJ*, 458, 257
- Gotthelf, E.V., Vasisht, G., Boylan-Kolchin, M., et al., 2000, *ApJ*, 542, L37
- Green, D.A., 2001, "A catalogue of Galactic Supernova Remnants (2001 December Version)", <http://www.mrao.cam.ac.uk/surveys/snrs/>
- Guseinov, O. Kh., Yerli, S. K., Özkan, S., Sezer, S., and Tagieva, S. O., 2002, 'Distances and Other Parameters for 1315 Radio Pulsars', submitted to *AN*
- Halpern, J.P., Camilo, F., Gotthelf, E.V., et al. 2001, *ApJ*, 552, L125
- Hamilton, A.J.S., Fesen, R.A., Wu, C.-C., et al. 1997, *ApJ*, 481, 838
- Hulse, R.A., Taylor, J.H., 1974, *ApJ*, 191, L59
- Hulse, R.A., Taylor, J.H., 1975, *ApJ*, 201, L55
- Johnston, S., Lyne, A.G., Manchester, et al. 1992a, *MNRAS*, 255, 401

Johnston, S., Manchester, R.N., Lyne, A.G., et al. 1992b, ApJ, 387, L37
 Johnston, S., Manchester, R.N., Lyne, A.G., et al. 1994, MNRAS, 268, 430
 Johnston, S., Walker, M.A., van Kerkwijk, M.H., et al. 1995, MNRAS, 274, L43
 Kaspi, V.M., Manchester, R.N., Johnston, S., et al. 1996, AJ, 111, 2028
 Kaspi, V.M., & Helfand, D.J., 2002, astro-ph/0201183v1
 Kassim, N.E., & Weiler, K.W., 1990, Nat., 343, 146
 Kulkarni, S.R., Anderson, S.B., 1996, in IAU SYmp. 174: Dynamical Evolution of Star Clusters: Confrontation of Theory and Observations, vol. 174, p. 181
 Lorimer, D.R., Bailes, M., Dewey, R.J., and Harrison, P.A., 1993, MNRAS, 263, 403
 Lorimer, D.R., Lyne, A.G., Camilo, F., 1998, A&A, 331, 1002
 Lyne, A., 1995, in ASP Conf. Ser, 72: Millisecond Pulsars: A Decade of Surprise, p. 35
 Lyne, A.G., Camilo, F., Manchester, R.N., et al. Stairs, I.H., 2000, MNRAS, 312, 698
 Lyne, A.G., Manchester, R.N., Lorimer, D.R., et al. , 1998, MNRAS, 295, 743
 Manchester, R.N., Lyne, A.G., D'Amico, N., et al. 1996, MNRAS, 279, 1235
 Manchester, R.N., Taylor, J.H., 1981, AJ, 86, 1953
 Marshall F.E., Gotthelf E.V., Zhang W. et al. 1998, ApJ 499, L179
 Mignani, R.P., Pulone L., Marconi G. et al. 2000, A&A, 355, 603
 Murray, S.S., Slane, P.O., Seward, F.D., et al. 2002, ApJ, in press (astro-ph/0108489)
 Ögelman, H., Koch-Miramond, L., Auriere, M., 1989, ApJ, 342, L83
 Pivovarovoff, M.J., Kaspi, V.M., Camilo, F., et al. 2001, ApJ, 554, 161
 Sandhu, J.S., Bailes, M., Manchester, R.N., , 1997, ApJ, 478, L95
 Shull, J.M., Fesen, R.A., and Saken, J.M., 1989, APJ, 346, 860
 Stokes, G.H., Segelstein, D.J., Taylor, J.H., Dewey, R.J., 1986, ApJ, 311, 694
 Stokes, G.H., Taylor, J.H., Welsberg, J.M., Dewey, R.J., 1985, Nat. 317, 787
 Strom, R.G., 1987, ApJ, 319, L103
 Taylor, J.H., Cordes, J.M., 1993, ApJ, 411, 674
 Taylor, J.H., Manchester, R.H., Lyne, A.G., Camilo, F., 1996, Catalog of 706 PSRs, unpublished work, an extended version of 1993, ApJS, 88, 529

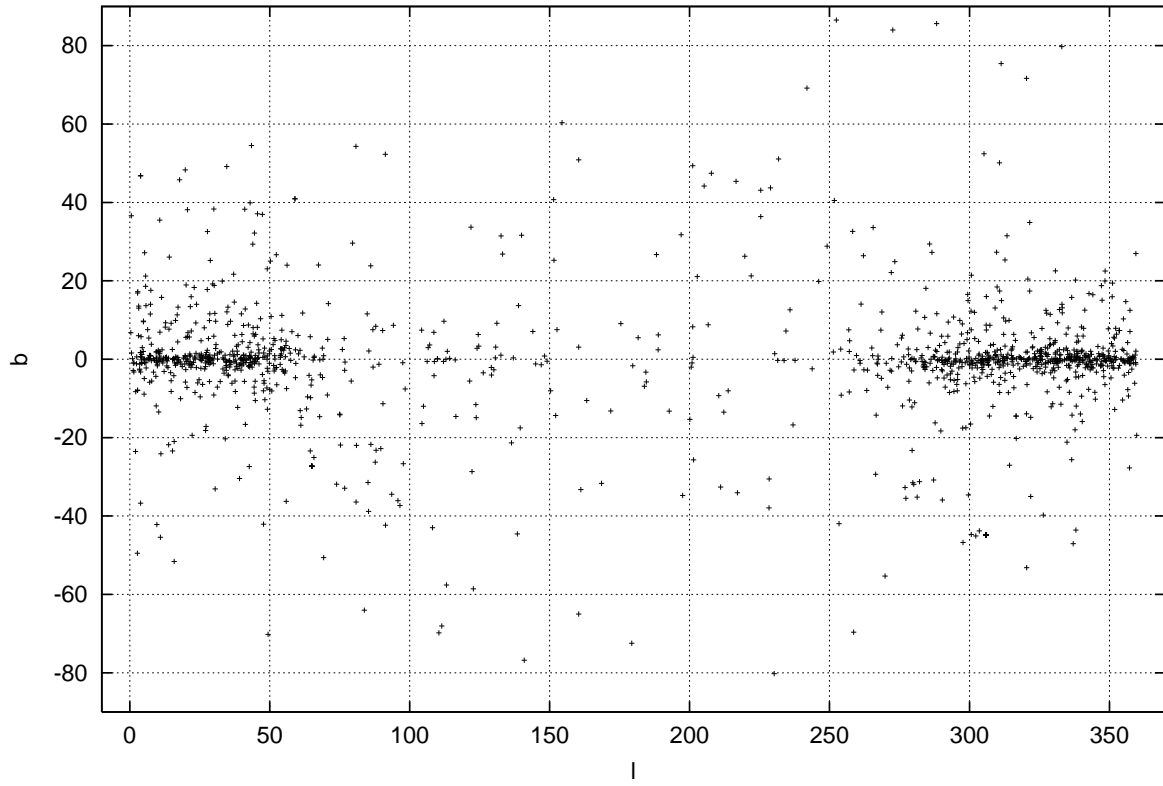


Figure 1a. Galactic longitude (l) versus Galactic latitude (b) of 1315 PSRs.

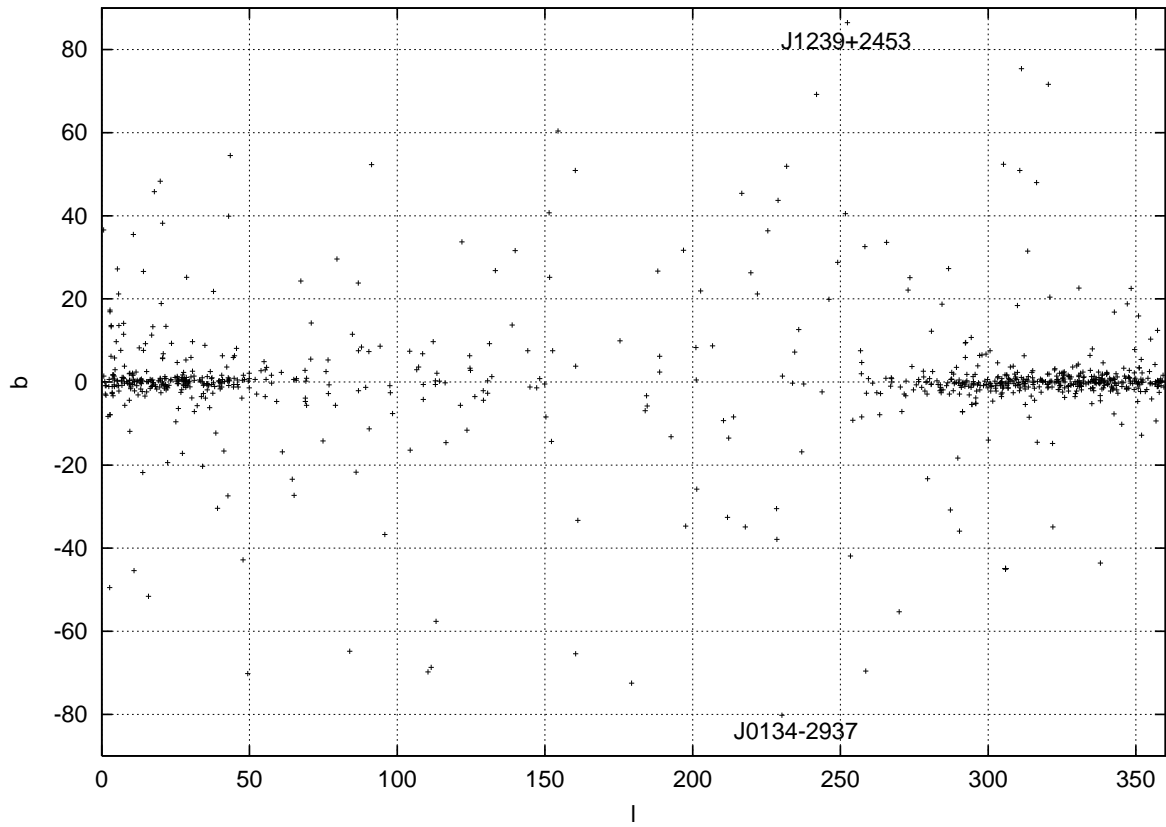


Figure 1b. The l - b distribution of 862 galactic PSRs which have flux measured at 1400 MHz.

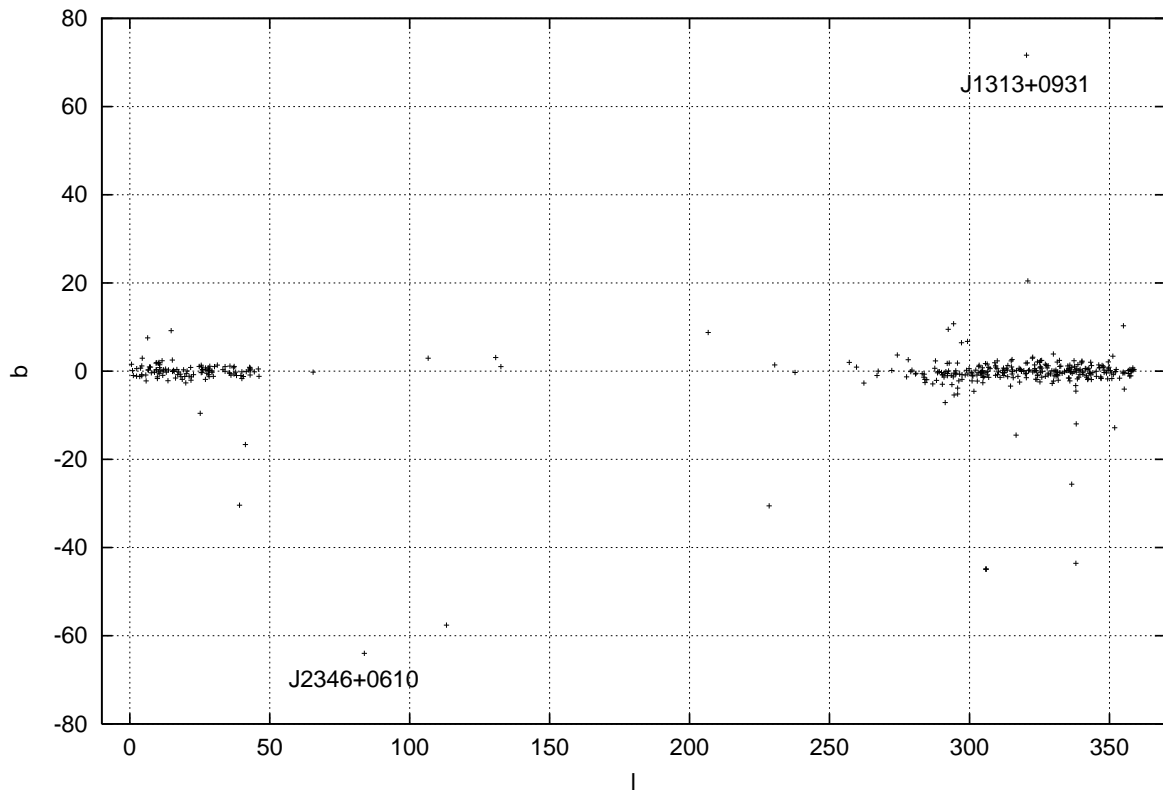


Figure 1c. The l - b distribution of 419 PSRs discovered after 1996 with flux measured at 1400 MHz

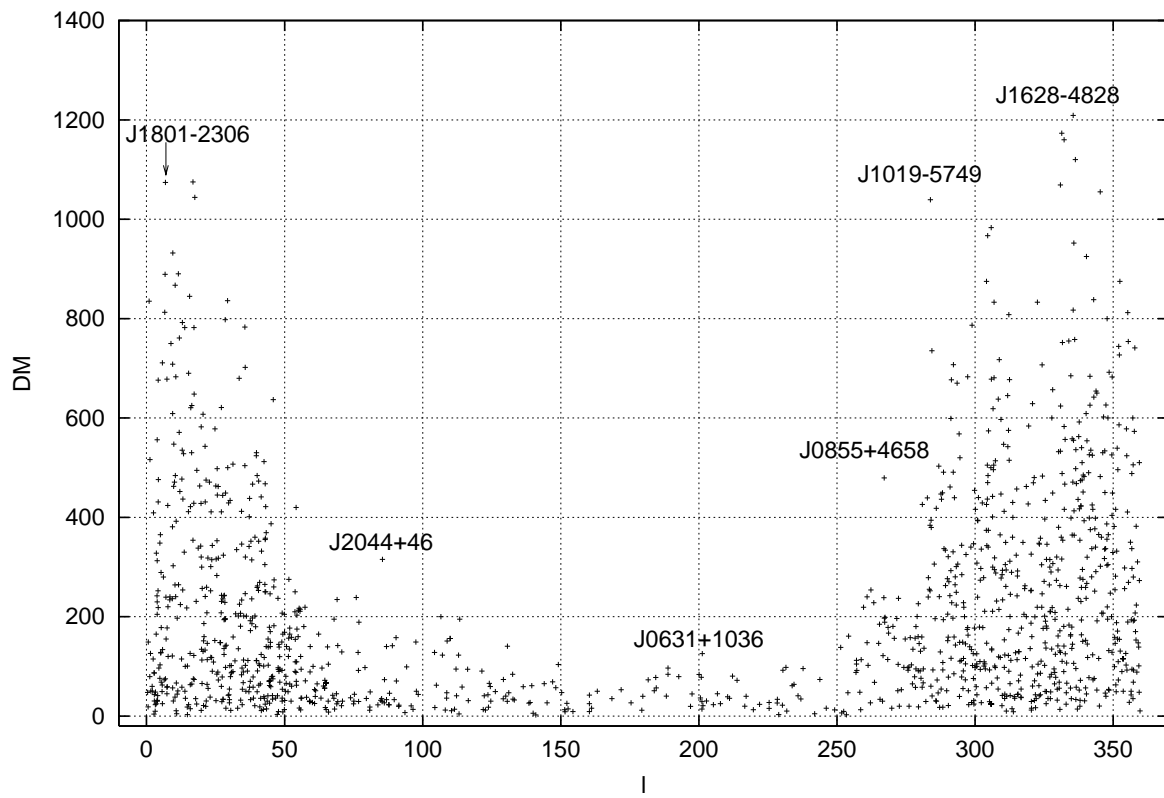


Figure 2a. DM values of 1312 PSRs in the Galaxy with respect to Galactic longitude.

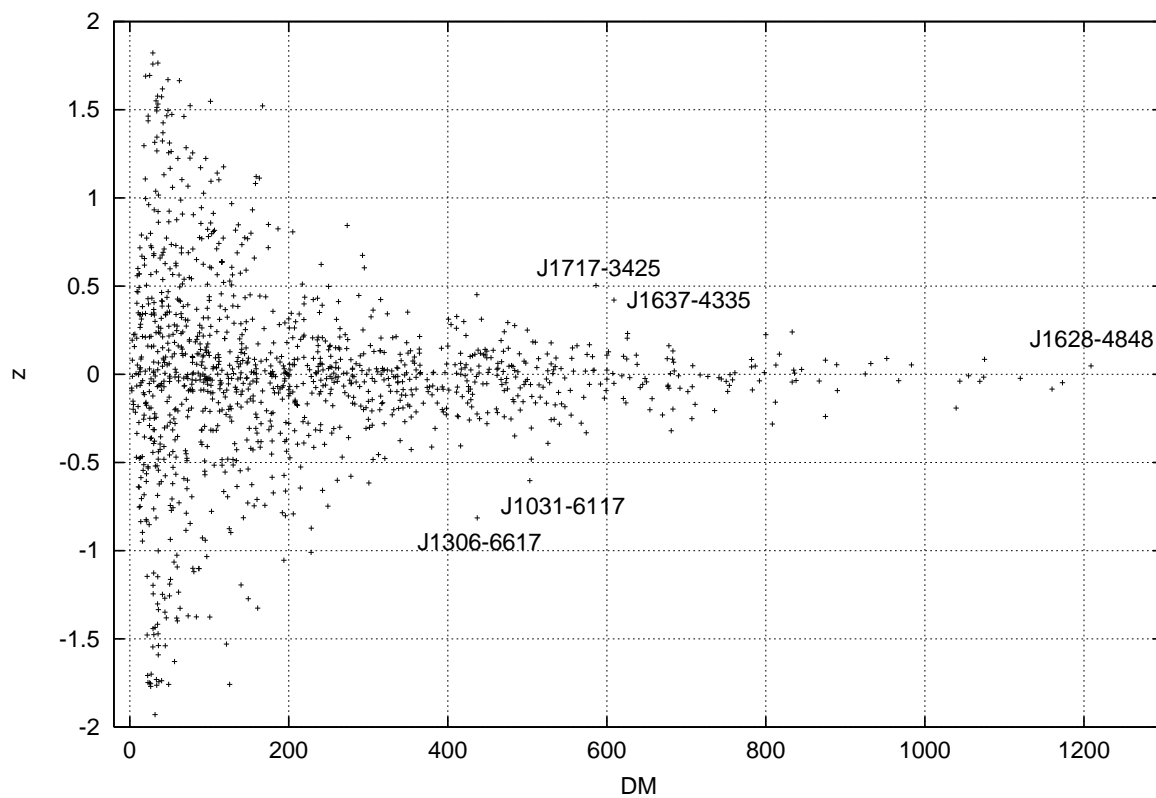


Figure 2b. The distance from the Galactic plane vs. DM for 1273 PSRs with $|Z| < 2$ kpc.

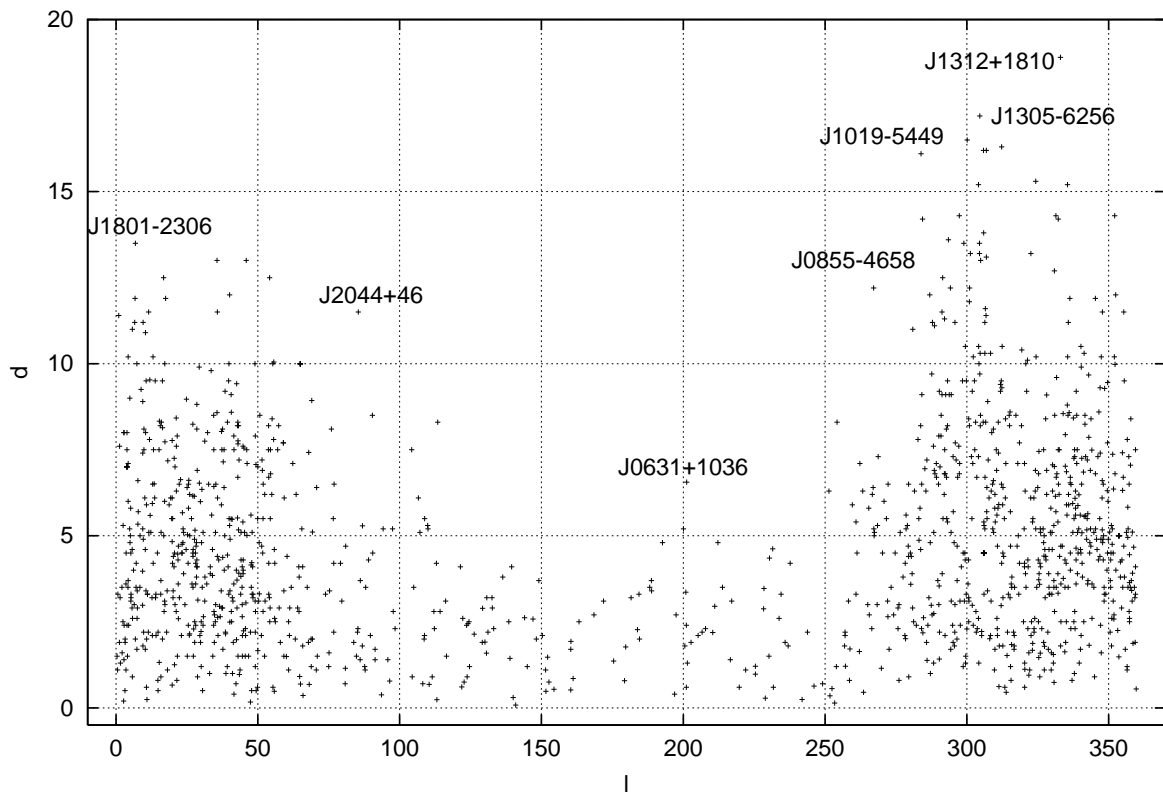


Figure 3a. The distances of 1307 PSRs which belong to our Galaxy versus Galactic longitude (d-l).

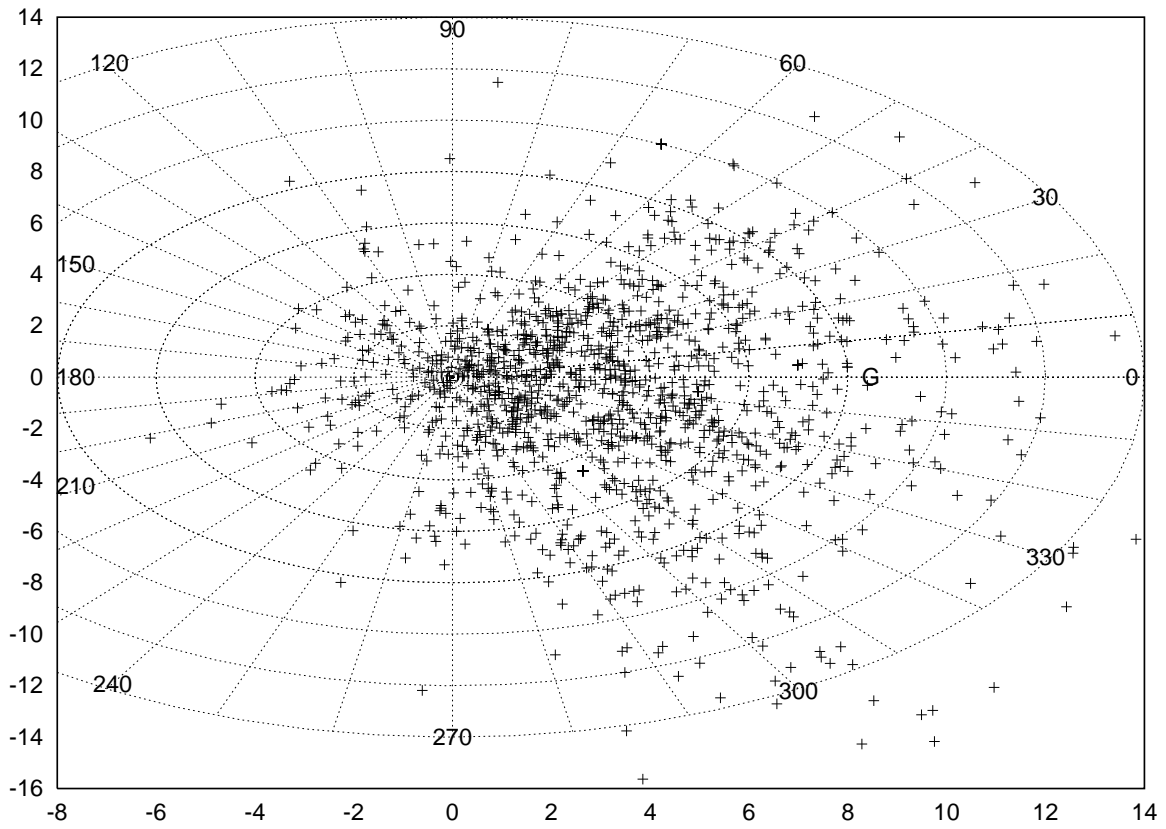


Figure 3b. The projection of the locations of PSRs on the plane of the Galaxy. G represents the galactic center.

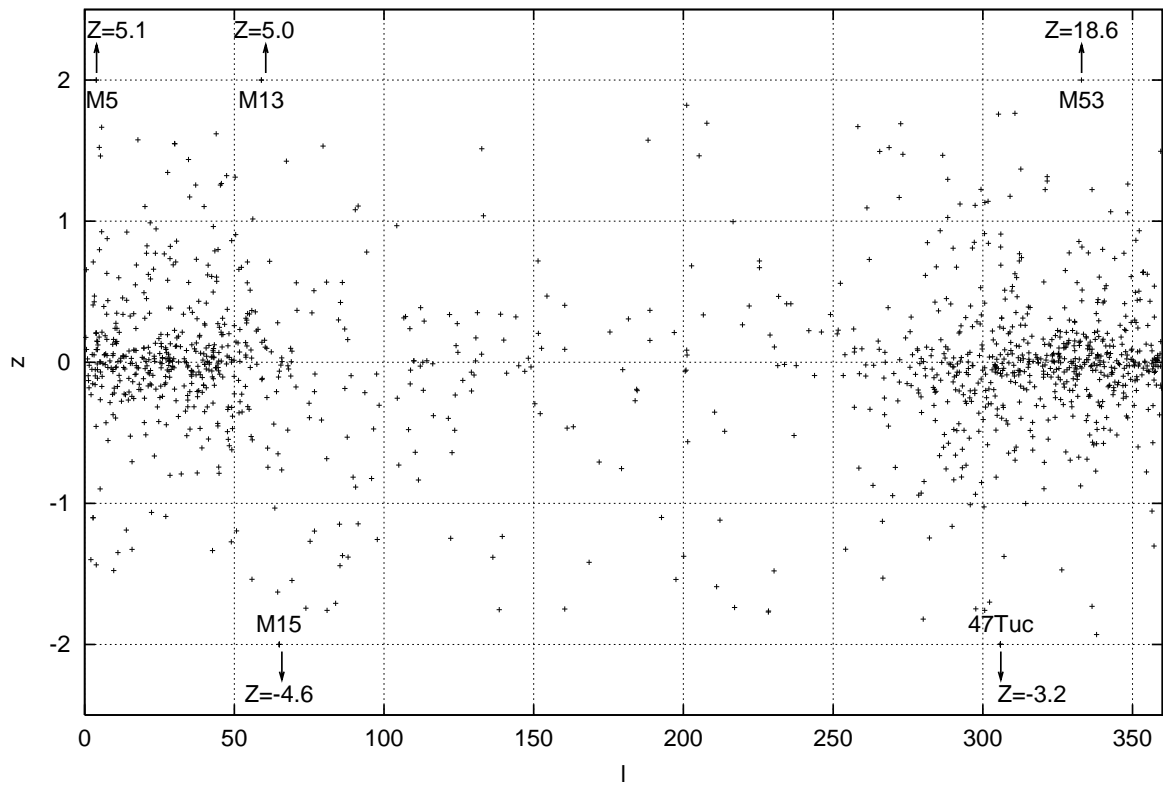


Figure 4a. The distribution of the distances of 1307 galactic PSRs from the plane of Galaxy as a function of galactic longitude.

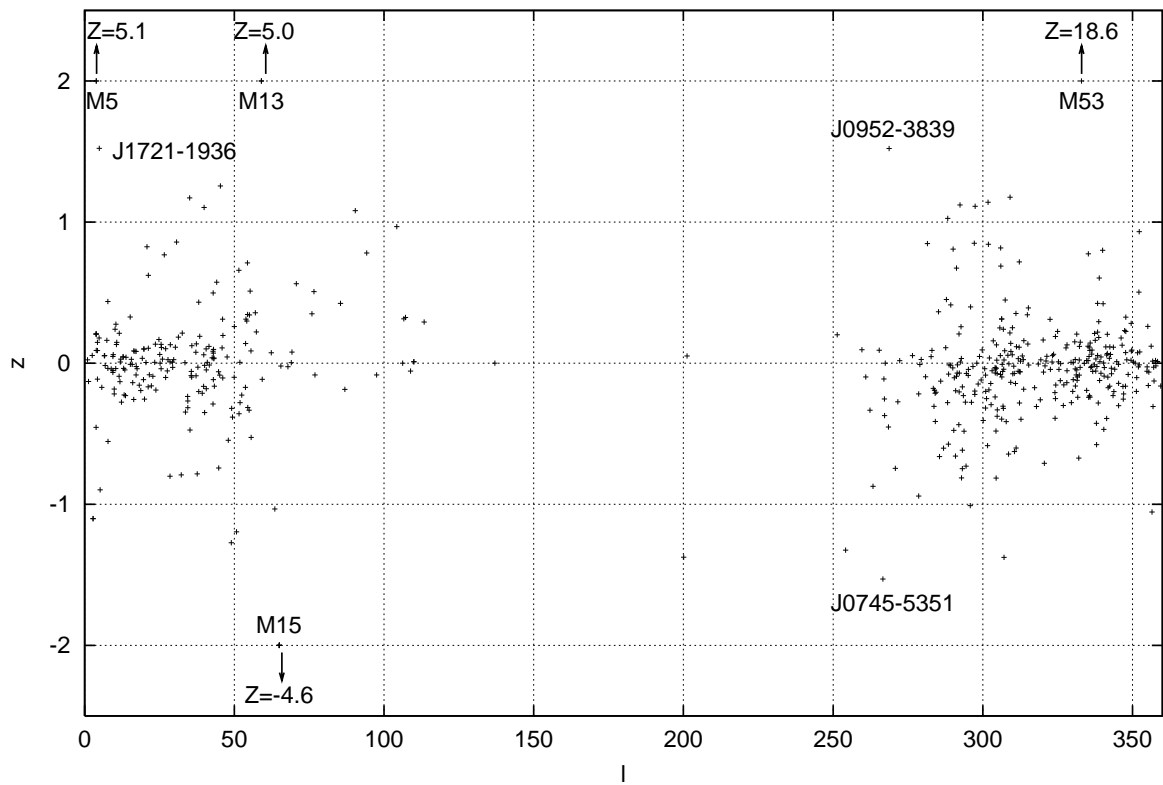


Figure 4b. Z - l distribution for 551 PSRs with distance more than 5 kpc.

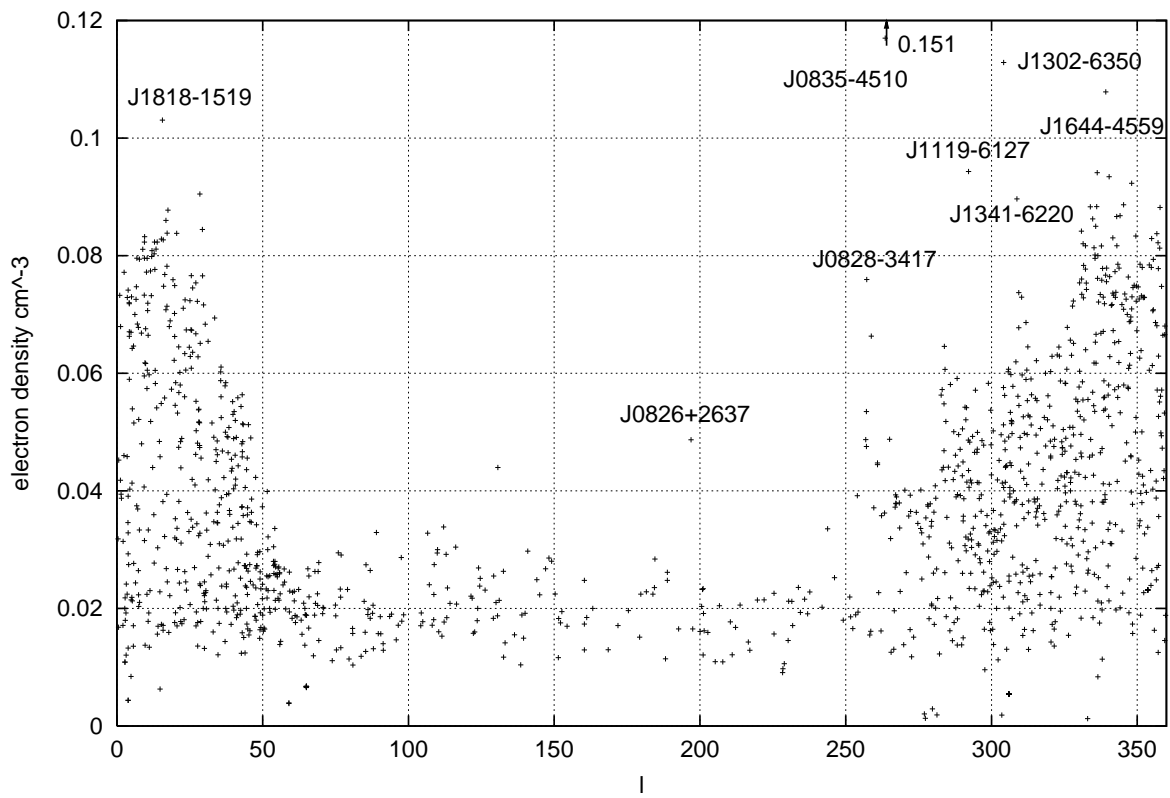


Figure 5. The average value of electron density, n_e , along the line of sight vs. Galactic longitude for 1312 PSRs

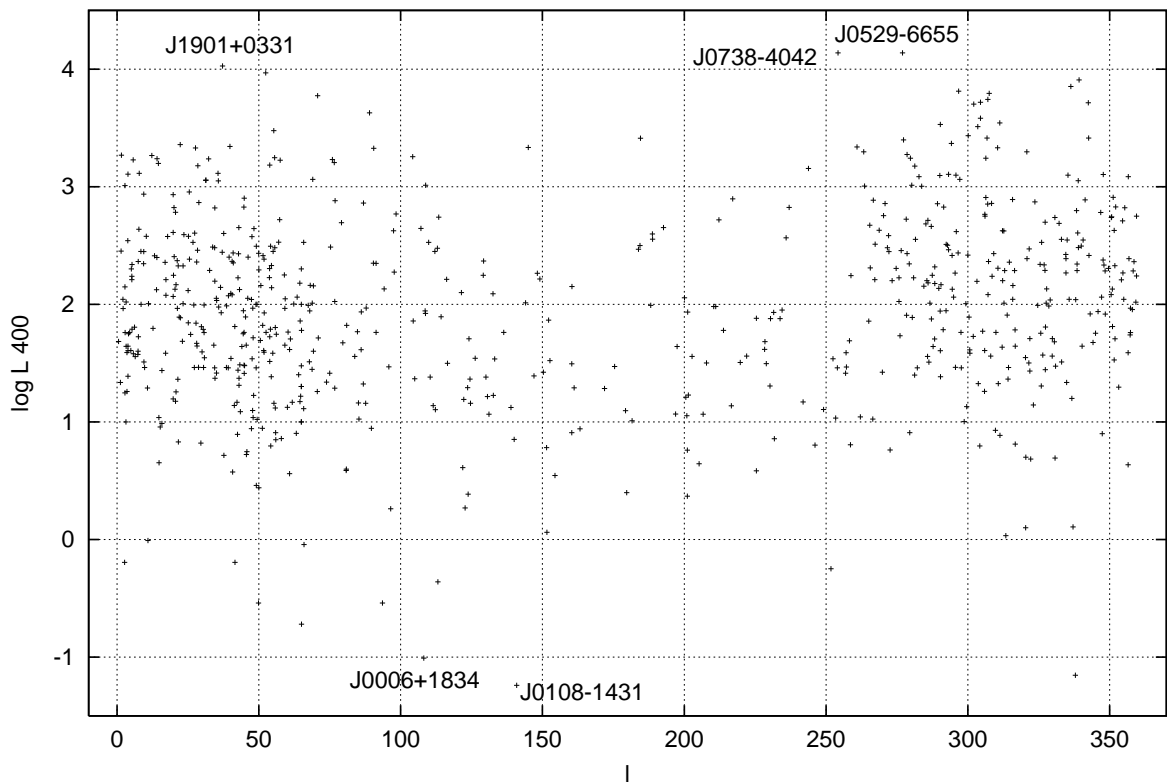


Figure 6a. The luminosity at 400 MHz ($L_{400}=F_{400}d^2$ mJy kpc²) vs. longitude of 685 Galactic PSRs.

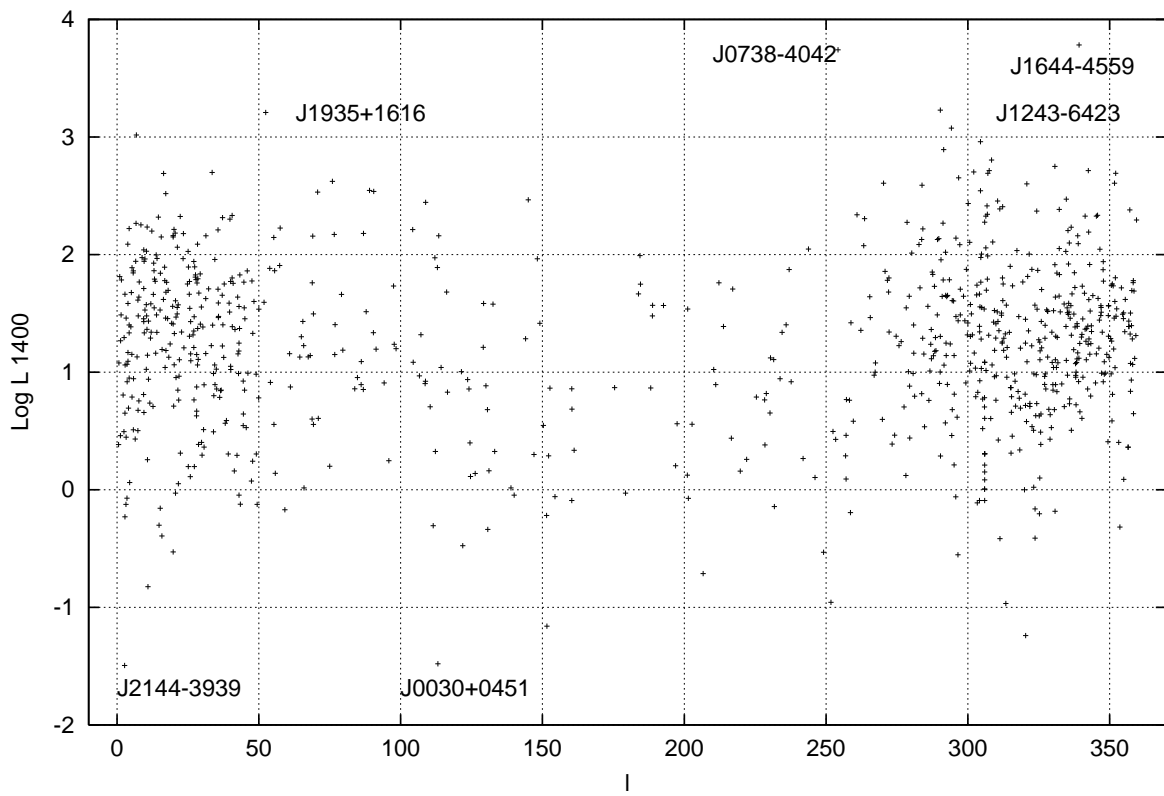


Figure 6b. The luminosity at 1400 MHz vs. longitude of 862 Galactic PSRs

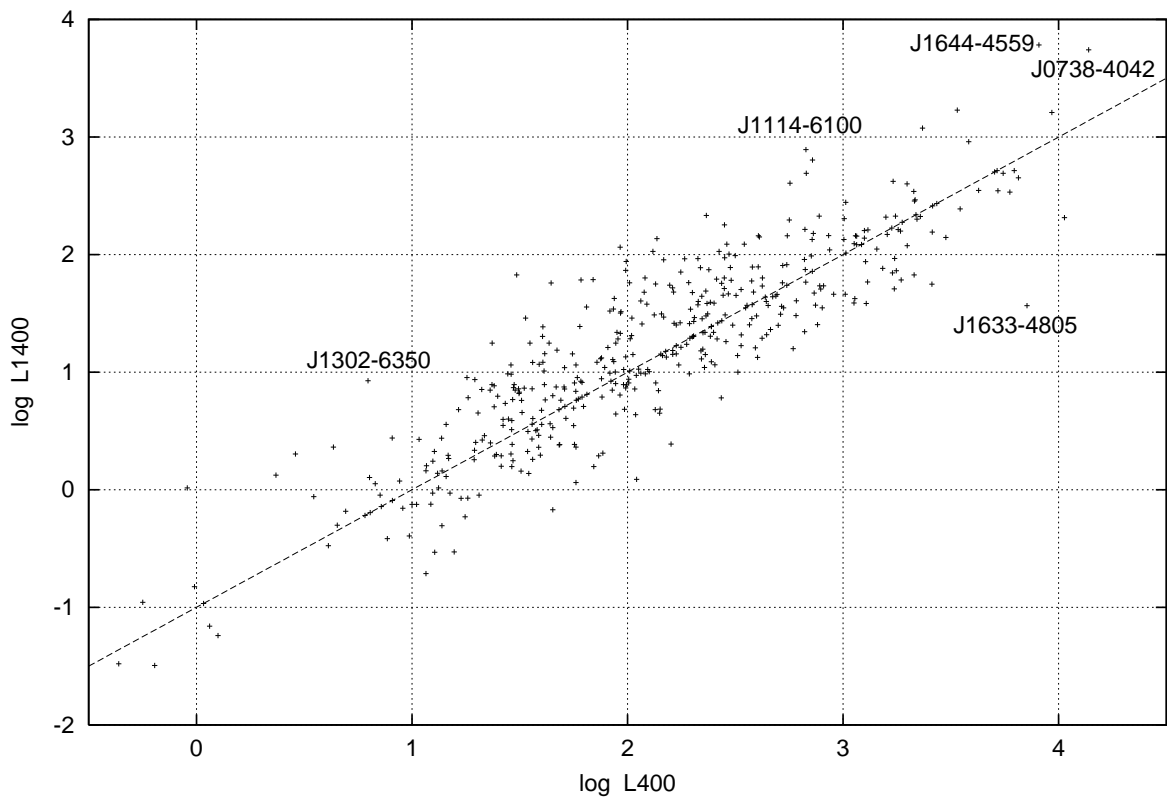


Figure 6c. The values of $\text{Log } L_{1400}$ vs. values $\text{Log } L_{400}$ for 449 PSRs

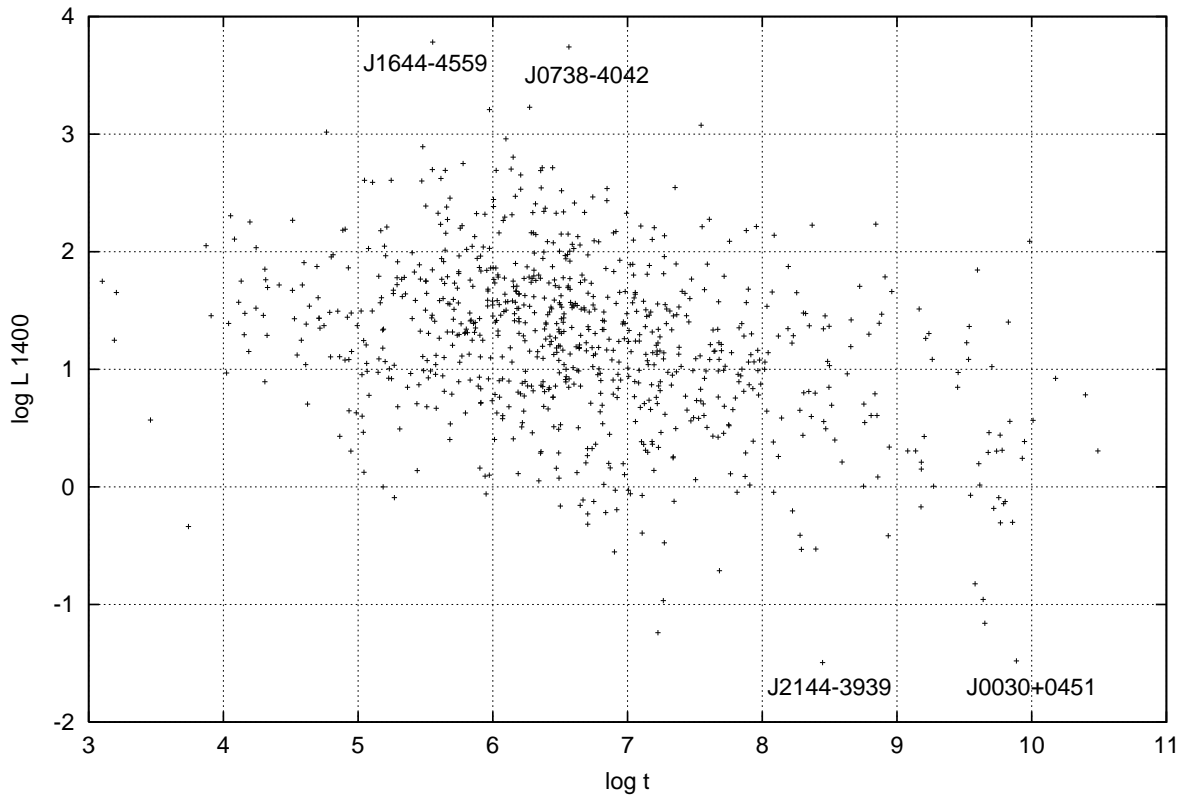


Figure 7a. Luminosities of PSRs at 1400 MHz as a function of characteristic age for 853 PSRs (5 PSRs in MC is included).

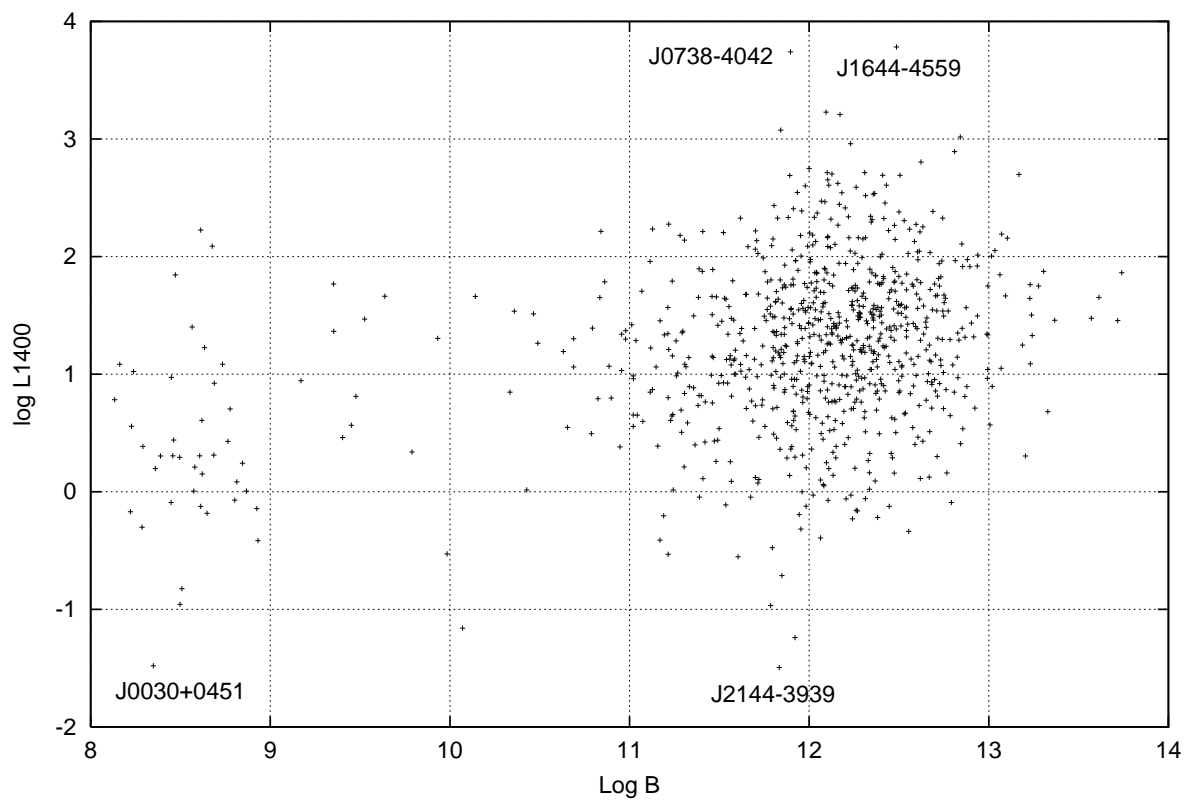


Figure 7b. Luminosity at 1400 MHz vs magnetic field for 853 PSRs.

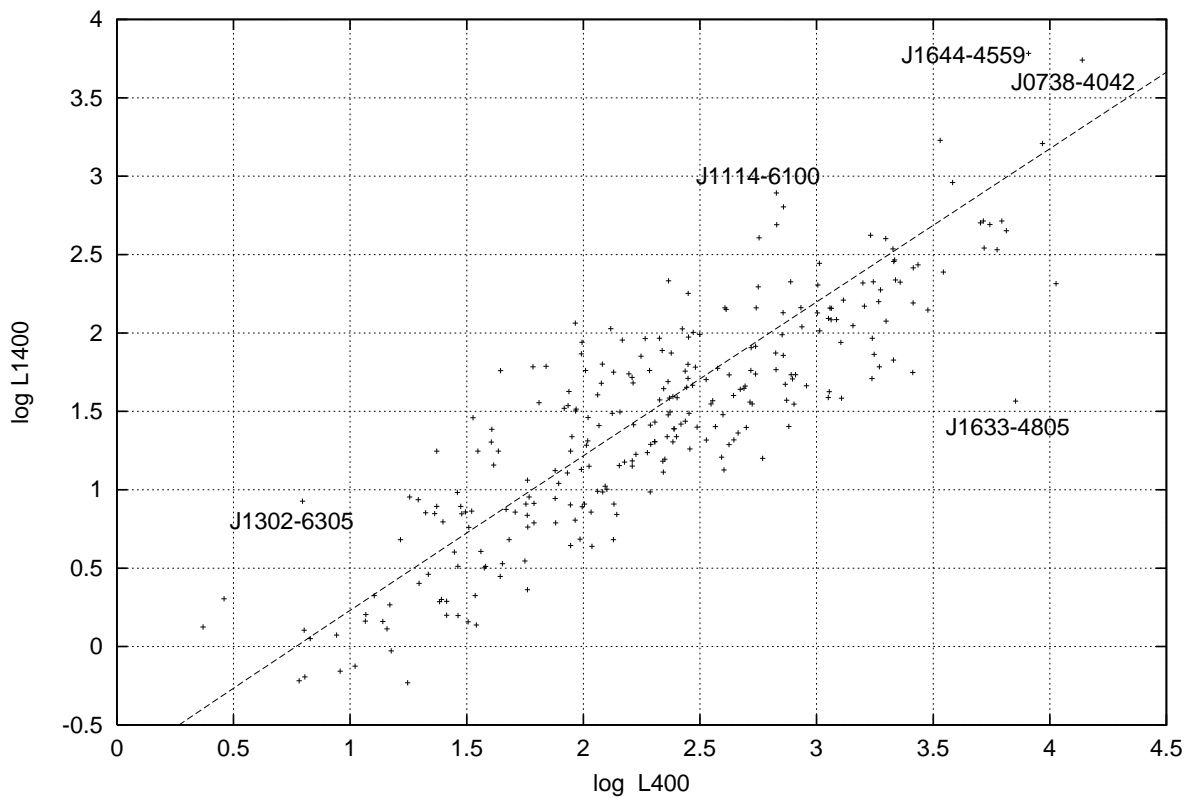


Figure 8a. $\log L_{1400}$ - $\log L_{400}$ diagram for 273 PSRs with $\tau < 10^7$ years.

Figure 8b. log L1400 - log L400 diagram for 93 PSRs with log T < 6 years

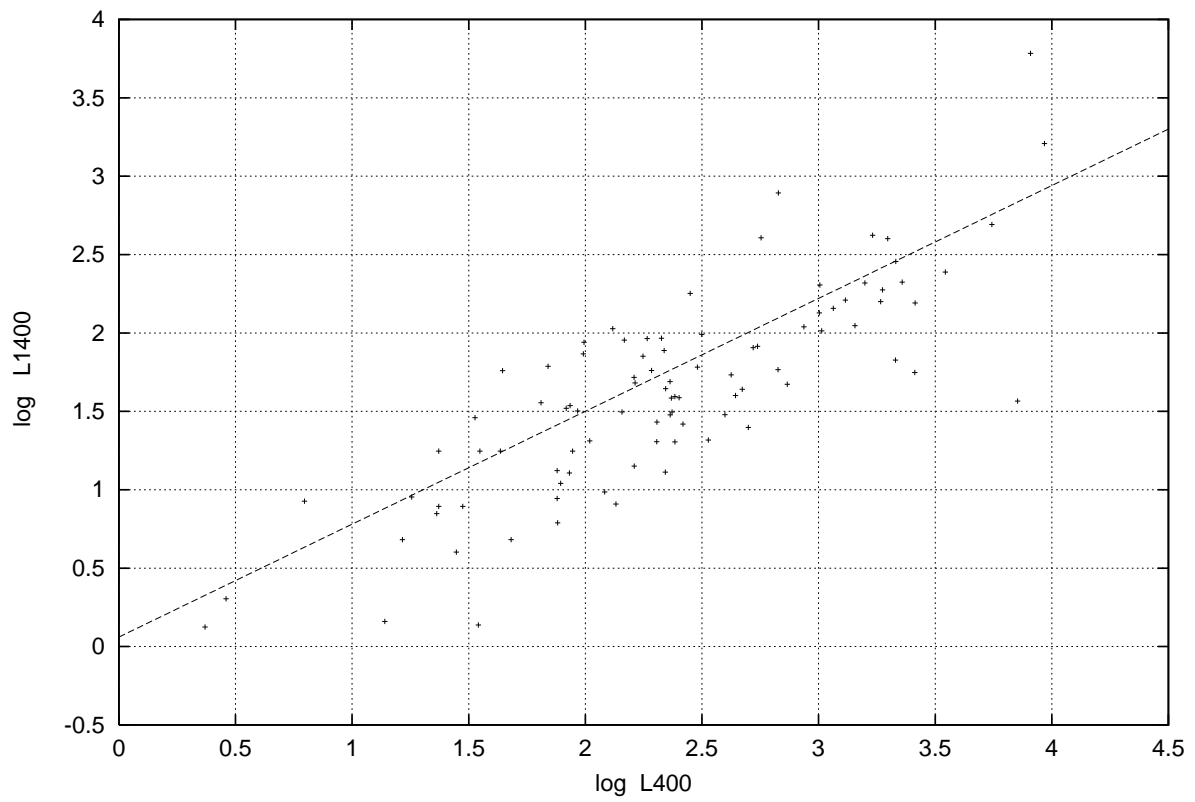


Figure 8b. Log L₁₄₀₀-Log L₄₀₀ diagram for 93 PSRs with $\tau < 10^6$ years.

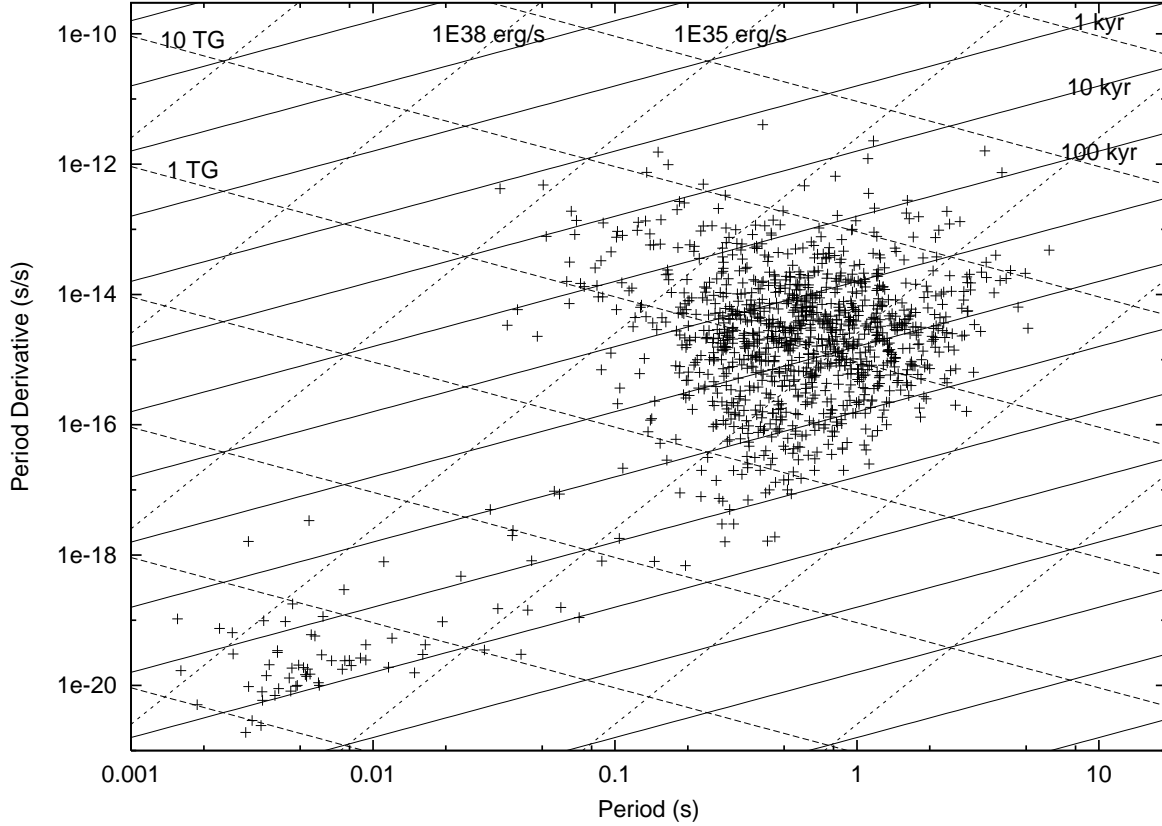


Figure 9. The $P-\dot{P}$ Diagram for 1191 PSRs. The constant characteristic age lines are given by the formula $\tau=P/2\dot{P}$, and the lines for 1, 10 and 100 kyr are indicated. The constant magnetic dipole field lines are given by the formula $B=3.3 \cdot 10^{19}(P\dot{P})^{1/2}$, and the lines for 1 and 10 TG are indicated. The constant rate of energy loss lines are given by the formula $\dot{E}=3.94 \cdot 10^{46}\dot{P}/P^3$ and the lines for 10^{38} and 10^{35} are indicated.